Prediction of the debulking effect of rotational atherectomy using optical frequency domain imaging

Tanimura, Kosuke ; Otake, Hiromasa ; Kawamori, Hiroyuki ; Toba, Takayoshi ; Nagasawa, Akira ; Sugizaki, Yoichiro ; Takeshige, Ryo ;…

(Citation)
Heart and Vessels,36(9):1265-1274

(Issue Date)
2021-04-08

(Resource Type)
journal article

(Version)
Accepted Manuscript

(URL)
https://hdl.handle.net/20.500.14094/0100477507

Prediction of the debulking effect of rotational atherectomy using optical frequency domain imaging

Author names and degrees:

Kosuke Tanimura, MD; Hiromasa Otake, MD, PhD; Hiroyuki Kawamori, MD, PhD; Takayoshi Toba, MD, PhD; Akira Nagasawa, MD; Yoichiro Sugizaki, MD, PhD; Ryo Takeshige, MD; Shinsuke Nakano, MD; Yoichiro Matsuoka, MD; Yu Takahashi, MD; Yusuke Fukuyama, MD; Ken-ichi Hirata, MD, PhD

Author affiliations and addresses:

Kobe University Graduate School of Medicine, Division of Cardiovascular Medicine, Department of Internal Medicine

7-5-1 Kusunoki-cho, Chuo-ku, Kobe, Hyogo 650-0017, Japan

Address for corresponding author:

Hiromasa Otake, MD, PhD, FACC

Kobe University Graduate School of Medicine, Division of Cardiovascular Medicine, Department of Internal Medicine

7-5-1 Kusunoki-cho, Chuo-ku, Kobe, Hyogo, 650-0017, Japan

Tel: 81-78-382-5846; Fax: 81-78-382-5859; E-mail: hotake@med.kobe-u.ac.jp

Abstract

Background: Whether predicting the rotational atherectomy (RA) effect based on the position of optical frequency domain imaging (OFDI) is accurate remains uncertain. The aim of this study is to evaluate the predictive accuracy of OFDI in identifying RA location and area.

Methods: Twenty-five patients who underwent RA with OFDI were included. On pre-RA OFDI images, a circle with the dimension of a Rota burr was drawn at the center of the OFDI catheter. The area where the circle overlapped with the vessel wall was defined as the predicted ablation area (P-area), and the actual ablated area (A-area) was measured. The predictive accuracy of OFDI was evaluated as follows: overlapped ablation area (O-area: overlapping P- and A-areas) divided by P-area = %Correct-area, and A-area − O-area divided by A-area = %Error-area. Cross-sections were separated into four categories based on the median values of %Correct- and %Error-area.

Results: Among 334 cross-sections, RA effects were confirmed in the predicted location in 87% of them. The median %Correct- and %Error-areas were 43.1% and 64.2%, respectively. Floppy wire, narrow lumen area, OFDI catheter close to the intima, and large arc of calcium were independently associated with good prediction (high %Correct-/ low %Error-areas). Non-left anterior descending lesions, OFDI catheter far from the wire, and OFDI catheter and wire far from the intima were associated with irrelevant ablation (low %Correct-/ high %Error-areas).

Conclusions: The accuracy of the OFDI-based predictions for RA effects was acceptable with regard to location, but not high with regard to area. Wire types, target vessels, and OFDI catheter and wire positions are important determinants for accurately predicting RA effect using pre-procedural OFDI.

Keywords: Rotational atherectomy; optical frequency domain imaging; debulking effect; prediction.

Abbreviations:

A-angle (area/volume), actual ablation angle (area/volume)

AUC, area under the curve

IVUS, intravascular ultrasound

IQR, interquartile range

LAD, left anterior descending artery

LCx, left circumflex artery

OFDI, optical frequency domain imaging

OR, odds ratio

O-angle (area/volume), overlapped ablation angle (area/volume)

P-angle (area/volume), predicted ablation angle (area/volume)

PCI, percutaneous coronary intervention

RA, rotational atherectomy

RCA, right coronary artery

ROC, receiver operating characteristic

%Correct-angle (area), percentage of correct ablation angle (area)

%Error-area, percentage of error ablation area

Introduction

With the aging population, the frequency of catheter treatment for older patients with severe coronary artery calcification lesions is increasing [1]. Percutaneous coronary intervention (PCI) for severely calcified lesions remains technically challenging due to difficulty with balloon/stent delivery and achieving optimal stent expansion. PCI for severely calcified lesions can be associated with an increased rate of procedural failure and sub-optimal post-procedural outcomes compared to PCI for non-calcified lesions [2]. A previous study has reported that aggressive PCI techniques for coronary calcification and stent optimization could reduce the incidence of target lesion revascularization or major adverse cardiac events [3].

Coronary rotational atherectomy (RA) is a potential treatment option for calcified lesions that can effectively ablate calcified plaques, thereby facilitating balloon/stent delivery and optimal stent expansion. Recently, the Japanese Association of Cardiovascular Intervention and Therapeutics revised the institution criteria for the use of RA, resulting to expanding institutions that can use RA for daily clinical practice. However, complications associated with RA procedures have been reported, such as perforation, slow-flow/no-reflow phenomena, and coronary artery dissection. Insufficient atherectomy for calcification might lead to future in-stent restenosis if insufficient stent expansion is achieved immediately after stent implantation. Therefore, intravascular imaging might be recommended to evaluate target lesions and the appropriate RA device size to avoid potential procedure-related complications.

Optical frequency domain imaging (OFDI) is one of the most powerful tools used to evaluate coronary calcification because it facilitates the evaluation of

longitudinal and circumferential calcium distributions. OFDI also evaluates the calcification severity based on its accurate measurements of thickness [4]. Additionally, the RA location and area can be predicted from the pathway of the OFDI catheter inside the coronary artery using pre-RA OFDI; however, no report has clearly showed their relation. Therefore, the present study aimed to evaluate whether RA location and area in calcified plaque could be predicted using pre-RA OFDI and to investigate factors associated with the prediction.

Material and methods

Study population and procedural protocol

This was a retrospective, single-center, observational study performed to evaluate the predictive accuracy of OFDI for RA. Patients who underwent PCI with RA for calcified lesions using OFDI at our institution from April 2010 to March 2019 were included. Patients whose OFDI images were not available or unanalyzable before and immediately after RA were excluded. We retrospectively collected data from patient records. Written informed consent was waived due to the retrospective nature of the study. The study protocol complied with the Declaration of Helsinki and was approved by the Ethical Committee of Kobe University Hospital.

RA was performed using the Rotalink Plus rotational atherectomy system (Boston Scientific Corporation, Natic, MA, USA) after exchanging the conventional 0.014-inch wire for the 0.009-inch RotaWire™ floppy guidewire (Boston Scientific Corporation) or RotaWire™ extra-support guidewire (Boston Scientific Corporation) using a micro-catheter. RA was performed according to standard practice [1] with a revolution speed of 180,000 or 200,000 rpm according to the operator's discretion.

Care was taken to avoid any decrease in rotational speed exceeding 5,000 rpm. The choice of starting speed, burr size, and wire type were dependent on the operator's discretion based on the European expert consensus regarding RA [1]. During RA procedure, a drug cocktail containing heparin, verapamil, and nitroglycerin was administered to prevent slow-flow and no-reflow phenomena.

OFDI imaging and analysis

An OFDI system (LUNAWAVE; Terumo, Tokyo, Japan) and OFDI catheter (Fast View; Terumo) were used for all cases. OFDI was performed before and after RA using a 0.014-inch conventional guidewire and 0.009-inch wire, respectively. For image acquisition, blood in the lumen was replaced with contrast media or low molecular dextran. An OFDI scan was performed from as far distal as possible to the ostium of each vessel including the entire length of the region of interest using an integrated automated pullback device at a rate of 40 mm/s using the standalone electronic control of the pullback motor.

Offline OFDI analysis was performed using a dedicated workstation (LUNAWAVE Offline Viewer; Terumo, Tokyo, Japan). The cross-sectional OFDI images were matched before and after RA based on the location of the intraplaque structure and side branches. In OFDI images after RA, the longitudinal target region of interest for OFDI analysis was set as the beginning to the end of the OFDI cross-sections where RA effects for calcification were visually confirmed. The matched longitudinal region on pre-RA OFDI images was set for OFDI analysis before RA.

The OFDI analysis was performed at 1-mm intervals by a dedicated

independent investigator (K.T.) blinded to the wire types used and target lesion locations. The predicted and actual ablated areas based on the OFDI catheter were defined according to the following criteria. On the pre-RA OFDI images, a circle of similar size to the dimensions of the Rota burr used was drawn in the center of the OFDI catheter. The area where the circle overlapped the vessel wall was defined as the predicted ablation area (P-area) (Figure 1A-1). The actual area ablated by RA was measured by superimposing the OFDI images before and after RA (A-area) (Figure 1A-2). The area where the P-area and A-area overlapped was defined as the overlapped ablation area (O-area) (Figure 1A-3). We also measured the angles of the P-, A-, and O-areas (P-angle, A-angle, and O-angle, respectively) around the center of the lumen on matched OFDI images (Figure 1A-4). P-, A-, and O-volume was calculated by integrating P-, A-, and O-area, respectively.

We measured the lumen area, arc of calcium, minimum thickness of calcium in the intima [5], minimum distance between the OFDI catheter and intima, minimum distance between the wire and intima, and minimum distance between the OFDI catheter and wire on each cross-section before RA. We also evaluated the presence of deep vessel wall injury extending beyond the media and intimal flap outside of the P-area in each cross-section (Figure 1B and C). All areas and distances were measured using Image J software (version 1.51W; U.S. National Institutes of Health, Bethesda, MD, USA). The length of calcium was determined by identifying the proximal and distal calcium edges and were summed if there were multiple separate calcium deposits. Calcium types were classified into three groups according to arc of calcium at the minimum lumen area (circumferential: an angle of calcification of 270° or more, eccentric: an angle of calcification of 270° or less, nodular: the protrusion of

calcification into the lumen) and the location of the eccentric and nodular calcifications were classified into myocardial and pericardial site based on the location of the intraplaque structure and side branches.

Categorical evaluation of the predictive accuracy of OFDI for RA effects

We evaluated the predictive accuracy of OFDI for RA effects in terms of RA location (area of ablation) and area (amount of ablation). For the position of the RA, the prediction accuracy was evaluated using %Correct-angle (O-angle divided by P-angle) (Figure 1A-4), which indicated how correct the predicted location was. The predictive accuracy of OFDI for RA area was evaluated using two parameters: %Correct-area (calculated as O-area divided by P-area): how correct the predicted area was, and %Error-area (calculated as A-area minus O-area divided by A-area): how much unexpectedly ablated the area was (Figure 1A-3). If there were cross-sections with the absence of A-area in post-RA OFDI images, these cross-sections were excluded due to the inability to analyze the %Error-area. As a volumetric analysis, %Correct-volume was calculated as O-volume divided by P-volume and %Error-volume was calculated as A-volume minus O-volume divided by A-volume.

All cross-sections were classified into four groups based on the median of the %Correct- and %Error-areas. In the good prediction group (high %Correct-/ low %Error-areas), the predicted RA effects were observed; in the over ablation group (high %Correct-/ high %Error-areas), larger than expected RA effects were observed; in the insufficient ablation group (low %Correct-/ low %Error-areas), RA was less

effective than expected; and in the irrelevant ablation group (low %Correct-/ high %Error-areas), RA effects were observed at locations different from those predicted.

Statistical analysis

Continuous variables with normal distributions are expressed as mean ± standard deviation. Variables with non-normal distributions are expressed as median and interquartile range (IQR, 25th–75th). A Student's t-test or analysis of variance was used to evaluate parametric continuous variables. A Mann–Whitney U test or Kruskal–Wallis test was used for non-parametric variables. Categorical variables are expressed as frequencies with percentage and compared using a χ^2 or Fisher's exact test. Logistic and multiple regression analyses were performed to identify independent factors with prediction. In the patient-based multivariate analysis, the first-treated lesion was used in patents who had multiple lesions registered. Variables of OFDI data with $P < 0.10$ in the univariate analysis were included in the multivariate analysis. The results are presented as odds ratios (OR) with 95% confidence intervals (CI). A two-sided $P < 0.05$ indicated statistical significance. All statistical analyses were performed using SPSS for Windows version 25 (IBM SPSS Inc., Armonk, NY, USA).

Results

Patient flow and baseline characteristics

Fifty-seven patients (58 lesions) underwent PCI with RA using OFDI. After excluding 32 patients (32 lesions), 25 patients (26 lesions) were enrolled and 334

cross-sections were analyzed (Supplementary Figure 1). Patient, lesion, and procedural characteristics are shown in Table 1.

Predictive accuracy of OFDI for the RA location

Among the 334 cross-sections, 23 were excluded because the circle with the Rota burr dimensions centered on the OFDI catheter did not overlap with the vessel wall (absence of the P-area). Regarding the predictive accuracy of the RA location, 105 of 311 cross-sections (33%) had a %Correct-angle of >80%, and 185 (59%) had a %Correct-angle of >50%. In contrast, 42 cross-sections (13%) had a %Correct-angle of 0%; thus, in those cross-sections, the RA location was completely different from what was predicted (Figure 2).

Lesion and patient-specific assessment, and associated factors with predictive accuracy of OFDI for RA volume

Lesion-based analyses are shown in Supplementary Table 1. Regarding the volumetric analysis, there was no difference between the median P-volume and the median A-volume (median, 6.08 [IQR, 3.52–10.59] mm^3 versus 6.39 [IQR, 3.54–12.36] mm3; $P = 0.241$). The median %Correct- and %Error-volumes were 50.3% and 67.0%, respectively. Multiple linear regression analysis for the patient-based factors independently associated with %Correct- and %Error-volume showed no such factors found to exist in this patient population (Supplementary Table 2).

Predictive accuracy of OFDI for RA areas and its impact on post-RA findings

Overall, the median P-area was significantly smaller than the median A-area (median, 0.47 [IQR, 0.20–0.74] mm^2 versus 0.54 [IQR, 0.28–0.74] mm^2; $P < 0.001$). The median %Correct- and %Error-areas were 43.1% and 64.2%, respectively (Table 2, Figure 3).

There was no significant difference in the median %Correct-area for floppy wire and extra-support wire use (46.4% vs. 52.5%, respectively; $P = 0.278$). However, the median %Error-area was significantly lower for floppy wire use than for extra-support wire use (55.6% vs. 65.7%, respectively; $P = 0.015$).

Similarly, there was no significant difference in the median %Correct-area among target vessels (left anterior descending [LAD] vs. left circumflex [LCx] vs. right coronary artery [RCA]: 49.8% vs. 50.7% vs. 41.9%, respectively; $P = 0.307$). The median %Error-area for LCx lesions was the highest among the target vessels (LAD vs. LCx vs. RCA: 53.7% vs. 75.3% vs. 63.4%, respectively; $P < 0.001$).

When all cross-sections were categorized based on the median values of the %Correct- and %Error-areas, cross-sections with a deep vessel wall injury extending beyond the media tended to be more frequently observed in the over ablation group (9.6%; P for χ^2 test = 0.160) than in the other groups. Those with the intimal flap outside of the P-area were more frequently observed in the irrelevant ablation group (18.1%; P for χ^2 test < 0.001) than in the other groups (Supplementary Figure 2).

Factors associated with the accuracy of OFDI-based RA effect prediction

The multivariate logistic regression analysis revealed that floppy wire use (OR, 2.59; 95% CI, 1.45–4.62; $P = 0.001$), the distance between the OFDI catheter and intima (OR, 0.01; 95% CI, 0.00–0.16; $P = 0.001$), the burr/lumen ratio (OR, 4.12;

95% CI, 1.71–10.1; $P = 0.002$), and the arc of calcium (OR, 1.00; 95% CI, 1.00–1.01; $P = 0.006$) were independently associated with good prediction (Table 3). Extra-support wire use (OR, 2.21; 95% CI, 1.17–4.16; $P = 0.014$) was independently associated with over ablation (Supplementary Table 3). Additionally, non-LAD lesions (OR, 0.54; 95% CI, 0.33-0.89; $P = 0.016$), the distance between the OFDI catheter and intima (OR, 30.4; 95% CI, 2.92–316.4; $P = 0.004$), the distance between the wire and intima (OR, 4.05; 95% CI, 1.15–14.3; $P = 0.03$), and the distance between the OFDI catheter and wire (OR, 44.3; 95% CI, 3.67–534.1; $P = 0.003$) were independently associated with irrelevant ablation (Table 4).

Figure 4A shows a representative case involving good prediction of a proximal LAD lesion, ablated by a 1.75-mm burr using floppy wire. Coronary angiography and cross-sectional OFDI images indicated that the wire was in contact with the OFDI catheter. OFDI showed that the RA was successfully performed near the same location as the predicted ablation area, based on the circles centered on the OFDI catheter. The mean %Correct- and %Error-areas for this case were 55% and 8%, respectively.

Figure 4B shows an additional representative case involving the irrelevant ablation of a middle RCA lesion, ablated by a 1.50-mm burr using extra-support wire. A non-contrast angiogram revealed that the OFDI catheter was far from the guidewire, especially at the minimum lumen site. OFDI showed that after RA, although the A-area almost overlapped with the P-area at the most distal site of the lesion where the OFDI catheter and extra-support wire were closely located, it almost did not overlap with the P-area in the other proximal cross-sections. However, OFDI after RA showed that the circles centered on the guidewire before RA closely overlapped with the A-

area (rather than the P-area). The mean %Correct- and %Error-areas for this case were 29% and 74%, respectively.

Discussion

Predictive accuracy of OFDI for RA

Although RA is useful for plaque modification in severe calcified lesions [1], several complications are potentially catastrophic [6] and effective measures to avoid such complications have not been established. Intravascular imaging methods are useful for evaluating coronary calcification and debulking effects [3, 7]. However, no study has systematically evaluated the predictive accuracy of imaging-based predictions of RA effects and factors associated with prediction.

In the present study, an angle-based analysis demonstrated that in 87% of cross-sections, at least part of the predicted region was ablated. More specifically, 33% of cross-sections had a %Correct-angle of >80%; thus, in 33% of analyzed cross-sections, >80% of predicted angle locations were ablated. One hundred and eighty-five cross-sections (59%) had a %Correct-angle of >50%, and 57 cross-sections (18%) had a %Correct-angle of 100%. Therefore, we consider that RA location can be predicted using the OFDI catheter pathway to some extent. Conversely, when taking the area into consideration, the median %Correct- and %Error-areas were 43.1% and 64.2%, respectively. In addition, the median %Correct- and %Error-volumes were 50.3% and 67.0%, respectively, suggesting that the predictive accuracy of OFDI catheter-based prediction for the amount of ablation was not high.

In general, physicians decide the indication of RA based on OFDI images before coronary intervention. If the OFDI catheter pathway is close to the target

calcium and apart from the thin normal vessel wall, then RA is considered safe to perform. However, insufficient prediction for the RA location sometimes occurs and insufficient area prediction was associated with unfavorable phenomena such as deep vessel wall injury extending beyond the media and the intimal flap outside of the P-area in the present study. Considering that these factors might lead to unfavorable RA complications (such as hematoma formation and coronary perforation), accurate prediction for RA effect and clarifying its associated factors are clinically important.

Potential factors associated with the prediction of RA effects with OFDI

In the present study, we characterized the predictive accuracy for RA according to the relationship between OFDI-based predictions and actual RA effects. Then, we clarified the factors associated with each category. In the patient-based, volumetric analysis, we demonstrated that no factor was independently associated with %Correct- and %Error-volume. Even within the same lesion, we can see a distinct variation of the OFDI findings (e.g., lumen area, morphology and distribution of calcification, and the location of wire and OFDI catheter) depending on the longitudinal location. Thus, we currently speculate that it might be difficult to find specific factors for predicting an RA effect based on the patient-based volumetric assessment. Indeed, in our daily practice, we usually perform cross-section-based OFDI assessment, since several catastrophic complications can be avoided only by detailed cross-section-based OFDI assessment. Thus, we adopted the cross-section-based assessment as a major analytical approach of the present study rather than lesion or patient-based one.

According to the multivariate logistic regression analysis of the cross-section

based analysis, floppy wire use, narrow lumen area compared with Rota burr size, and the OFDI catheter close to the intima were independently associated with good prediction. In general, the floppy wire could follow coronary artery angulation better than the extra-support wire, resulting in better predictions of RA effects with OFDI. Additionally, an OFDI catheter close to the intima can be suggestive of RA bias toward the direction. Finally, the narrow lumen area compared with Rota burr size and OFDI catheter being in contact with the intima were good indicators of the RA device moving less within the stenotic lesions. Therefore, OFDI-guided prediction of the ablation area could be accurate under these conditions.

Alternatively, extra-support wire use was independently associated with over ablation. The extra-support wire passes through a coronary artery by straightening an arterial curvature. Therefore, target lesions could be deeply ablated with an extra-support wire, especially when lesions are tortuous. Consequently, the incidence of deep vessel wall injury extending beyond the media was the most observed in over ablation groups than others.

In contrast, non-LAD lesions, OFDI catheter and wire far from the intima, and OFDI catheter far from the wire were independently associated with irrelevant ablation. Non-LAD lesions contain tortuous or bifurcation lesions more often than LAD lesions. In these cases, the OFDI catheter and wire were occasionally separated (Figure 4B). Since the Rota burr passes over the wire (not the OFDI catheter), the OFDI catheter-based prediction was less accurate; therefore, wire-based (not OFDI catheter-based) predictions might be helpful if the OFDI catheter and guidewire are far apart.

Wire types, target vessels, and positions of the OFDI catheter and wire can be

important for accurately predicting RA effects with pre-procedural OFDI. OFDI-guided RA might help to reduce RA-related complications during coronary intervention for calcified lesions. Further prospective studies are necessary to confirm our findings.

Limitations

The present study had several limitations. First, this study was a single-center, retrospective, observational study with a small sample size. Also, the exclusion rate was relatively high mainly due to the cases in which the OFDI catheter could not pass before RA. Therefore, a selection bias likely exists. Second, only patients who underwent RA with OFDI were enrolled in order to avoid the difference in imaging catheter types affecting the results. Thus, it remains unclear whether the present results could be applicable to the other optical coherence tomography system. Third, several important parameters, such as RA speed, number, and guiding catheter position were not unified, and some data were missing. Regarding RA speed, the relation between RA speed and debulking area is still controversial. [8, 9]. In the present study, RA was performed with a high revolution speed (180,000 or 200,000 rpm) in all cases. Thus, we currently consider that the impact of RA speed on the principal findings is minimum, if any. Forth, the reproducibility of the wire position on pre-RA OFDI was not unclear, because there were no cases in which multiple OFDI scans were performed before RA. Fifth, our analyses were based on cross-sections. Lesion length was proportional to the number of cross-sections, which may have created a bias. Sixth, the longitudinal target region of interest for OFDI analysis was set as the beginning to the end of the OFDI cross-sections where RA effects were visually confirmed.

Thus, %Correct-area might be overestimated by excluding cross-sections without A-area. Finally, because no complications occurred, the relationship between complication rate and predictive accuracy of OFDI for RA effects remains uncertain.

Conclusions

We demonstrated that although prediction of the RA location is feasible, accurate prediction, especially of the extent of RA effects, might be difficult using the OFDI catheter pathway. Wire types, target vessels, and positions of the OFDI catheter and wire should be studied further to determine their importance regarding predictive accuracy.

Declarations

Conflict of interest

The authors declare that they have no conflict of interest.

Funding

This research received no grant from any funding agency in the public, commercial, or not-for-profit sectors.

Acknowledgments

None.

Consent to participate

Written informed consent was waived due to the retrospective nature of the study.

Ethics approval

The study protocol complied with the Declaration of Helsinki and was approved by

the Ethical Committee of Kobe University Hospital.

References

1. Barbato E, Carrie D, Dardas P, Fajadet J, Gaul G, Haude M, Khashaba A, Koch K, Meyer-Gessner M, Palazuelos J, Reczuch K, Ribichini FL, Sharma S, Sipotz J, Sjogren I, Suetsch G, Szabo G, Valdes-Chavarri M, Vaquerizo B, Wijns W, Windecker S, de Belder A, Valgimigli M, Byrne RA, Colombo A, Di Mario C, Latib A, Hamm C, European Association of Percutaneous Cardiovascular Interventions (2015) European expert consensus on rotational atherectomy. EuroIntervention 11:30–36
2. Lee MS, Shah N (2016) The impact and pathophysiologic consequences of coronary artery calcium deposition in percutaneous coronary interventions. J Invasive Cardiol 28:160–167
3. Shan P, Mintz GS, Witzenbichler B, Metzger DC, Rinaldi MJ, Duffy PL, Weisz G, Stuckey TD, Brodie BR, Genereux P, Croiwley A, Kirtane AJ, Stone GW, Maehara A (2017) Does calcium burden impact culprit lesion morphology and clinical results? An ADAPT-DES IVUS substudy. Int J Cardiol 248:97–102
4. Kume T, Okura H, Kawamoto T, Yamada R, Miyamoto Y, Hayashida A, Watanabe N, Neishi Y, Sadahira Y, Akasaka T, Yoshida K (2011) Assessment of the coronary calcification by optical coherence tomography. EuroIntervention 6:768–772
5. Maejima N, Hibi K, Saka K, Akiyama E, Konishi M, Endo M, Iwahashi N, Tsukahara K, Kosuge M, Ebina T, Umemura S, Kimura K (2016) Relationship between thickness of calcium on optical coherence tomography and crack formation after balloon dilatation in calcified plaque requiring rotational atherectomy. Circ J 80:1413–1419

6. Sakakura K, Inohara T, Kohsaka S, Amano T, Uemura S, Ishii H, Kadota K, Nakamura M, Funayama H, Fujita H, Monomura SI (2016) Incidence and determinants of complications in rotational atherectomy: insights from the National Clinical Data (J-PCI Registry). Circ Cardiovasc Interv 9:e004278
7. Saita T, Fujii K, Hao H, Imanaka T, Shibuya M, Fukunaga M, Miki K, Tamaru H, Horimatsu T, Nishimura M, Sumiyoshi A, Kawakami R, Naito Y, Kajimoto N, Hirota S, Masuyama T (2017) Histopathological validation of optical frequency domain imaging to quantify various types of coronary calcifications. Eur Heart J Cardiovasc Imaging 18:342–349
8. Mizutani K, Hara M, Nakao K, Yamaguchi T, Okai T, Nomoto Y, Kajio K, Kaneno Y, Yamazaki T, Ehara S, Kamimori K (2020) Association between debulking area of rotational atherectomy and platform revolution speed-Frequency domain optical coherence tomography analysis. Catheter Cardiovasc Interv 95:E1-E7.
9. Kobayashi N, Yamawaki M, Hirano K, Araki M, Sakai T, Sakamoto Y, Mori S, Tsutsumi M, Sahara N, Nauchi M, Honda Y (2020) Additional debulking efficacy of low-speed rotational atherectomy after high-speed rotational atherectomy for calcified coronary lesion. Int J Cardiovasc Imaging. 36:1811-1819.

Figure Legends

Figure 1. Definition process of predicted and actual ablation according to OFDI before and after rotational atherectomy and a representative case of OFDI findings following rotational atherectomy.

(A) Definition process of the predicted and actual ablation areas. Cross-sectional OFDI image (1) before and (2) after RA. (3, 4) Superimposed OFDI images of before and after RA. The blue dotted line area indicates the predicted ablation area (P-area). The yellow dotted line indicates the actual ablation area (A-area). White circle indicates the Rota burr size circle (1.75 mm). (3) The red dotted line indicates where the P-area and A-area overlapped (O-area). (4) Blue, yellow, and red angles indicate the P-, R-, and O-angles, respectively. (B) Deep vessel wall injury extending beyond the media before (1) and after RA (2). Blue area indicates P-area. Yellow area indicates A-area. White circle indicates the Rota burr size circle (1.50 mm). Asterisks show deep vessel wall injury extending beyond the media following RA on above image. (C) Intimal flap outside of P-area (1) before and (2) after RA. White arrowhead indicates intimal flap outside of the P-area following RA. White circle indicates the Burr size circle (2.00 mm). OFDI, optical frequency domain imaging; RA, rotational atherectomy.

Figure 2. Distribution of %Correct-angle.

Figure 3. Distribution of %Correct- and %Error-areas in all cross-sections.

All cross-sections were plotted according to %Correct- and %Error-areas. The median %Correct- and %Error-areas were 43.1% and 64.2%, respectively. %Correct-

area, the ratio of correctness area; %Error-area, the ratio of error area.

Figure 4. Representative angiography and OFDI of good prediction and irrelevant ablation cases.

(A) Good prediction. (B) Irrelevant ablation. Angiography images with (upper left) and without contrast (lower left) are shown. OFDI results before and after rotational atherectomy are shown (right). White double-head arrow indicates target lesions. White triangles indicate wire position. White circles indicate the circle with Rota burr dimensions. Blue dotted line indicates the predicted ablation area (P-area). Yellow dotted line indicates the actual ablation area (A-area). The green dotted area indicates the P-area with wire-based prediction. (A) In the leftmost cross-sections, P- and A-area were measured as 0.89 mm^2 and 0.86 mm^2, respectively, and O-area (where overlapped P- and A-area) was 0.86 mm^2. The %Correct- and %Error-area were calculated to be 96.6% (O-area / P-area×100) and 0% ([A-area − O-area / A-area]×100), respectively. After conducting similar measurement and calculation on each cross-section, the mean %Correct-and %Error-area for each lesion were calculated by the sum of %Correct-and %Error-area for each cross-section divided by the number of cross-sections of the lesion. The mean %Correct- and %Error-area were calculated to be 55% and 8%, respectively. (B) The mean %Correct- and %Error-areas were 29% and 74%, respectively. OFDI, optical frequency domain imaging; RA, rotational atherectomy; P-area, predicted ablation area; A-area, real ablation area.

Table 1. Patient, lesion, and procedural characteristics

	Overall
Patients, n	25
Age, yrs	70.5 ± 10.1
Male, n (%)	20 (80)
Comorbidities	
Hypertension, n (%)	20 (80)
Diabetes mellitus, n (%)	14 (56)
Dyslipidemia, n (%)	19 (76)
Chronic kidney disease, n (%)	15 (60)
Hemodialysis, n (%)	6 (24)
Diagnosis	
Stable angina pectoris, n (%)	25 (100)
Acute coronary syndrome, n (%)	0 (0)
Lesion, n	26
Cross-section, n	334
Target vessel	
LAD, n (%)	15 (58)
LCx, n (%)	6 (23)
RCA, n (%)	5 (19)
Target lesion	
Proximal, n (%)	13 (50)
Mid, n (%)	11 (42)
Distal, n (%)	2 (8)
Approach site	
Transfemoral, n (%)	17 (65)
Transradial, n (%)	9 (35)
Guiding catheter type	
Judkins, n (%)	6 (23)
Extra back up, n (%)	13 (50)
Amplatzer, n (%)	7 (27)
Rotawire type	
Floppy wire, n (%)	16 (62)
Extra-support wire, n (%)	10 (38)
Burr size	
1.50 mm, n (%)	15 (58)

1.75 mm, n (%)	9 (34)
2.00 mm, n (%)	1 (4)
2.15 mm, n (%)	1 (4)
QCA analysis	
Lesion length, mm	19.9 (17.5–22.8)
Reference diameter, mm	2.77 (2.20–3.18)
MLD, mm	1.06 (0.83–1.26)
%Diameter stenosis, %	60.5 (47.5–67.1)
Burr-to-artery ratio	0.47 (0.39–0.53)

Values are expressed as median (interquartile range) or n (%). Abbreviations: LAD, left anterior descending; LCx, left circumflex; MLD, minimum lumen diameter; RCA, right coronary artery.

Table 2. OFDI measurements before and after rotational atherectomy according to cross-section-based analysis

	Overall
Pre/post-operative lumen measurements	**n=334**
Pre minimum lumen diameter, mm	1.62 (1.19–2.08)
Pre mean lumen diameter, mm	1.90 (1.53–2.48)
Pre lumen area, mm²	2.84 (1.84–4.88)
Burr/pre lumen ratio	0.88 (0.65–1.09)
Post minimum lumen diameter, mm	2.01 (1.67–2.28)
Post mean lumen diameter, mm	2.39 (2.01–2.71)
Post lumen area, mm²	4.48 (3.17–5.76)
Morphology of calcification	**n=334**
Arc of calcium, °	154.9 (97.3–257.4)
Minimum depth of calcium, μm	800 (540–1080)
Circumferential calcification, n (%)	104 (31.1)
Eccentric calcification, n (%)	123 (36.8)
Nodular calcification, n (%)	107 (32.0)
Location of myocardial site, n (%)	157 (68.2)
Location of pericardial site, n (%)	73 (31.8)
RA-related measurement	
Angle-based analysis	**n=311**
P-angle, ˚	127.1 (65.3–218.7)
A-angle, ˚	102.9 (70.6–142.3)
O-angle, ˚	64.6 (23.9–118.1)
%Correct-angle, %	55.3 (22.6–90.1)
Area-based analysis	**n=334**
P-area, mm²	0.47 (0.20–0.74)
A-area, mm²	0.54 (0.28–0.99)
O-area, mm²	0.18 (0.05–0.35)
%Correct-area, %	43.1 (14.9–69.4)
%Error-area, %	64.2 (31.4–90.4)
OFDI and wire position	**n=334**
Minimum distance between the OFDI catheter and intima, mm	0.001 (0–0.155)
Minimum distance between the wire and intima, mm	0.20 (0.10–0.33)
Minimum distance between the OFDI catheter and wire, mm	0.02 (0–0.05)

OFDI findings following RA	**n=334**
Deep vessel wall injury extending beyond media, n (%)	14 (4.2)
Intimal flap outside of the P-area, n (%)	26 (7.8)

Values are expressed as median (interquartile range) or n (%). Burr/lumen ratio was calculated by dividing the Rota burr size by the mean lumen diameter. %Correct-angle was calculated as O-angle divided by P-angle. %Correct-area was calculated as O-area divided by P-area. %Error-area was calculated as A-area minus O-area divided by A-area. Abbreviations: RA, rotational atherectomy; OFDI, optical frequency domain imaging; P-area, predicted ablation area; A-area, actual ablation area; O-area, overlap ablation area; P-angle, angle of predicted ablation area; A-angle, angle of actual ablation area; O-angle, angle of overlap ablation area; %Correct-angle (area), percentage of correct ablation angle (area); %Error-area, percentage of error ablation area.

Table 3. Univariate and multivariate logistic regression analyses according to the good prediction group

Variables	Univariate			Multivariate		
	OR	95% CI	*P* value	OR	95% CI	*P* value
LAD	1.99	1.21 – 3.29	0.007			
Floppy wire	1.86	1.12 – 3.09	0.016	2.59	1.45 – 4.62	0.001
Judkins type guiding catheter	0.89	0.49 – 1.61	0.692			
Pre lumen area	0.70	0.60 – 0.81	<0.001			
Burr / lumen ratio	8.17	3.61 – 18.5	<0.001	4.12	1.71 – 10.1	0.002
Distance between the OFDI catheter and intima	0.00	0.00 – 0.03	<0.001	0.01	0.00 – 0.16	0.001
Distance between the wire and intima	0.18	0.05 – 0.65	0.008			
Distance between the OFDI catheter and wire	0.03	0.001 – 0.61	0.024			
Myocardial site calcification	0.69	0.43 – 1.08	0.104			
Arc of calcium	1.00	1.00 – 1.01	0.006	1.00	1.00 – 1.01	0.006
Thickness of calcium	0.72	0.43 – 1.22	0.22			

Abbreviation: LAD, left anterior descending; OFDI, optical frequency domain imaging.

Table 4. Univariate and multivariate logistic regression analyses according to the irrelevant ablation group

Variables	Univariate			Multivariate		
	OR	95% CI	P value	OR	95% CI	P value
LAD	0.49	0.31 – 0.79	0.003	0.54	0.33 – 0.89	0.016
Extra-support wire	1.38	0.86 – 2.21	0.18			
Judkins type guiding catheter	1.25	0.70 – 2.23	0.45			
Pre lumen area	1.26	1.12 – 1.42	<0.001			
Burr / lumen ratio	0.13	0.05 – 0.31	<0.001			
Distance between the OFDI catheter and intima	154.7	19.6 – 1221	<0.001	30.4	2.92 – 316.4	0.004
Distance between the wire and intima	7.46	2.36 – 23.5	0.001	4.05	1.15 – 14.3	0.03
Distance between the OFDI catheter and wire	206.7	11.5 – 3279	<0.001	44.3	3.67 – 534.1	0.003
Myocardial site calcification	0.97	0.62 – 1.53	0.903			
Arc of calcium	1.00	0.99 – 1.003	0.53			
Thickness of calcium	1.47	0.87 – 2.49	0.15			

Abbreviation: LAD, left anterior descending; OFDI, optical frequency domain imaging.

Figure 1.

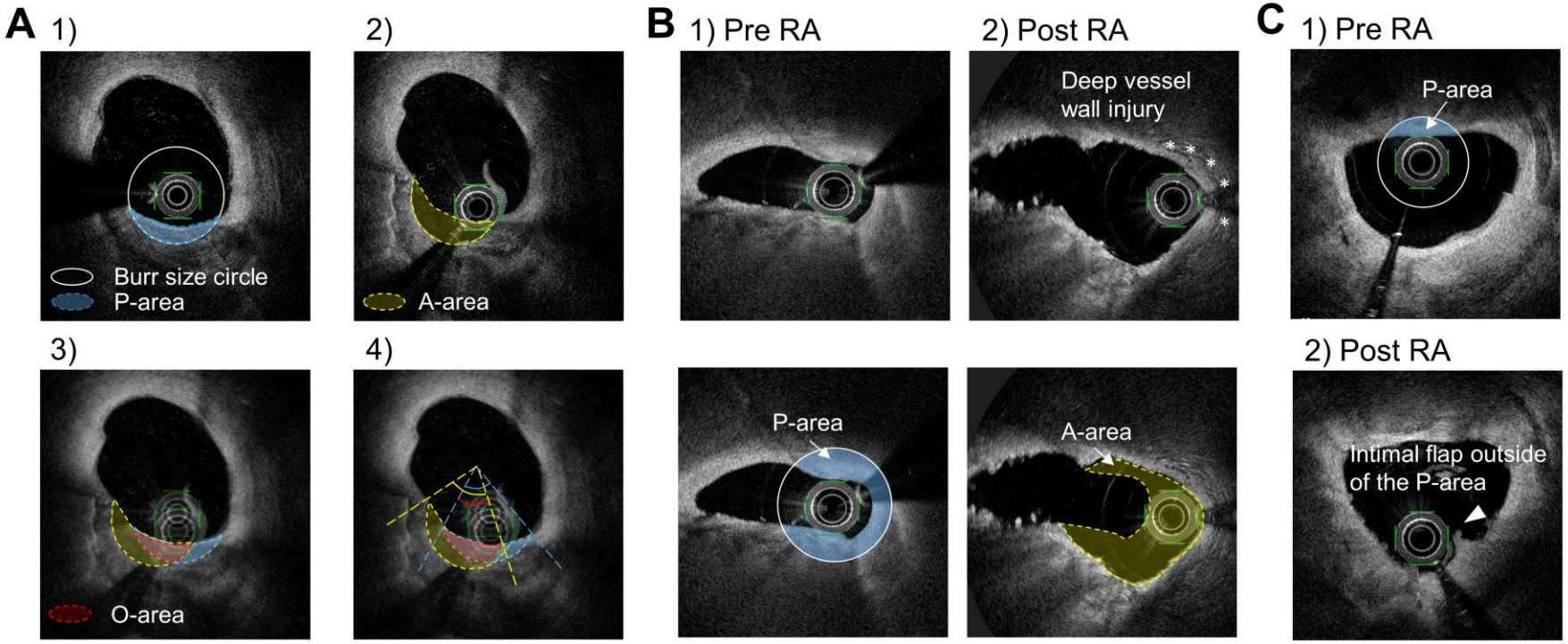
A
1)
2)
Burr size circle
P-area
A-area
3)
4)
O-area
B
1) Pre RA
2) Post RA
Deep vessel
wall injury
P-area
A-area
C
1) Pre RA
P-area
2) Post RA
Intimal flap outside
of the P-area

Figure 2.

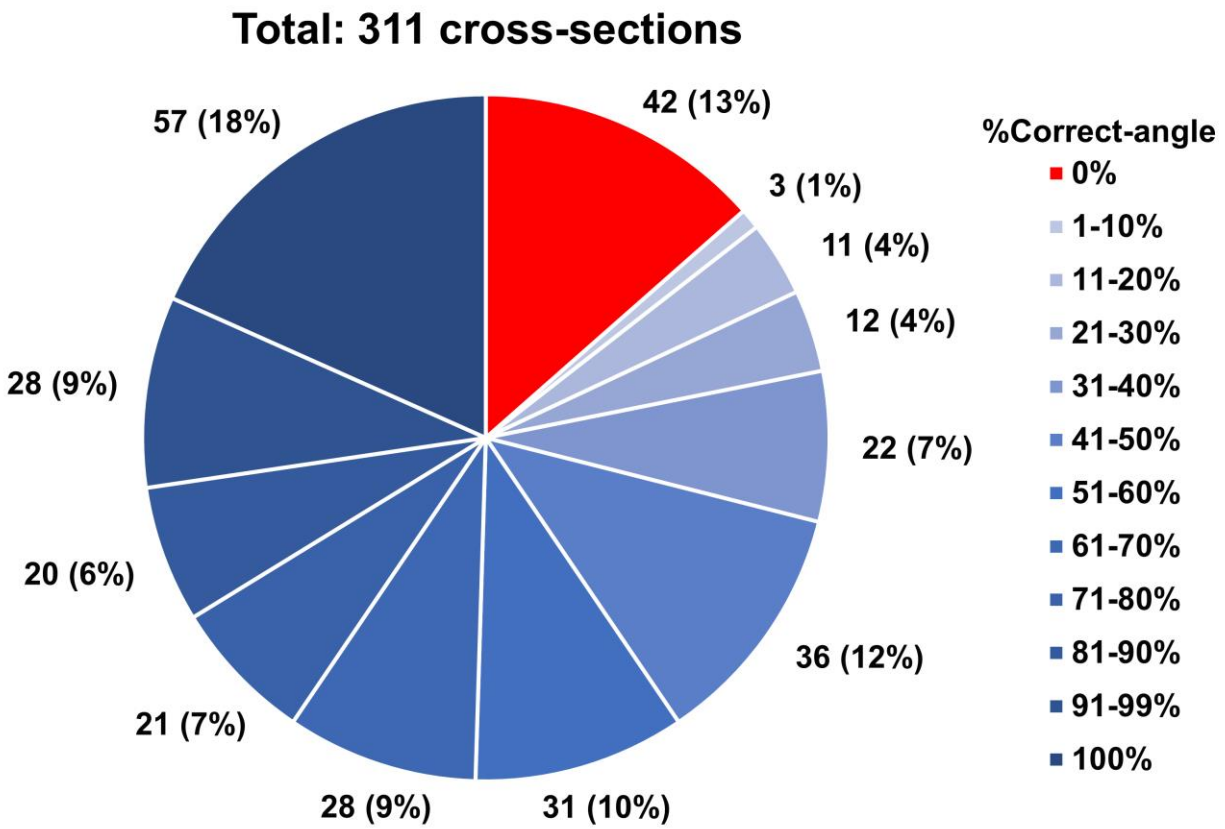
Total: 311 cross-sections
42 (13%)
3 (1%)
11 (4%)
12 (4%)
22 (7%)
36 (12%)
31 (10%)
28 (9%)
21 (7%)
20 (6%)
28 (9%)
57 (18%)
%Correct-angle
0%
1-10%
11-20%
21-30%
31-40%
41-50%
51-60%
61-70%
71-80%
81-90%
91-99%
100%

Figure 3.

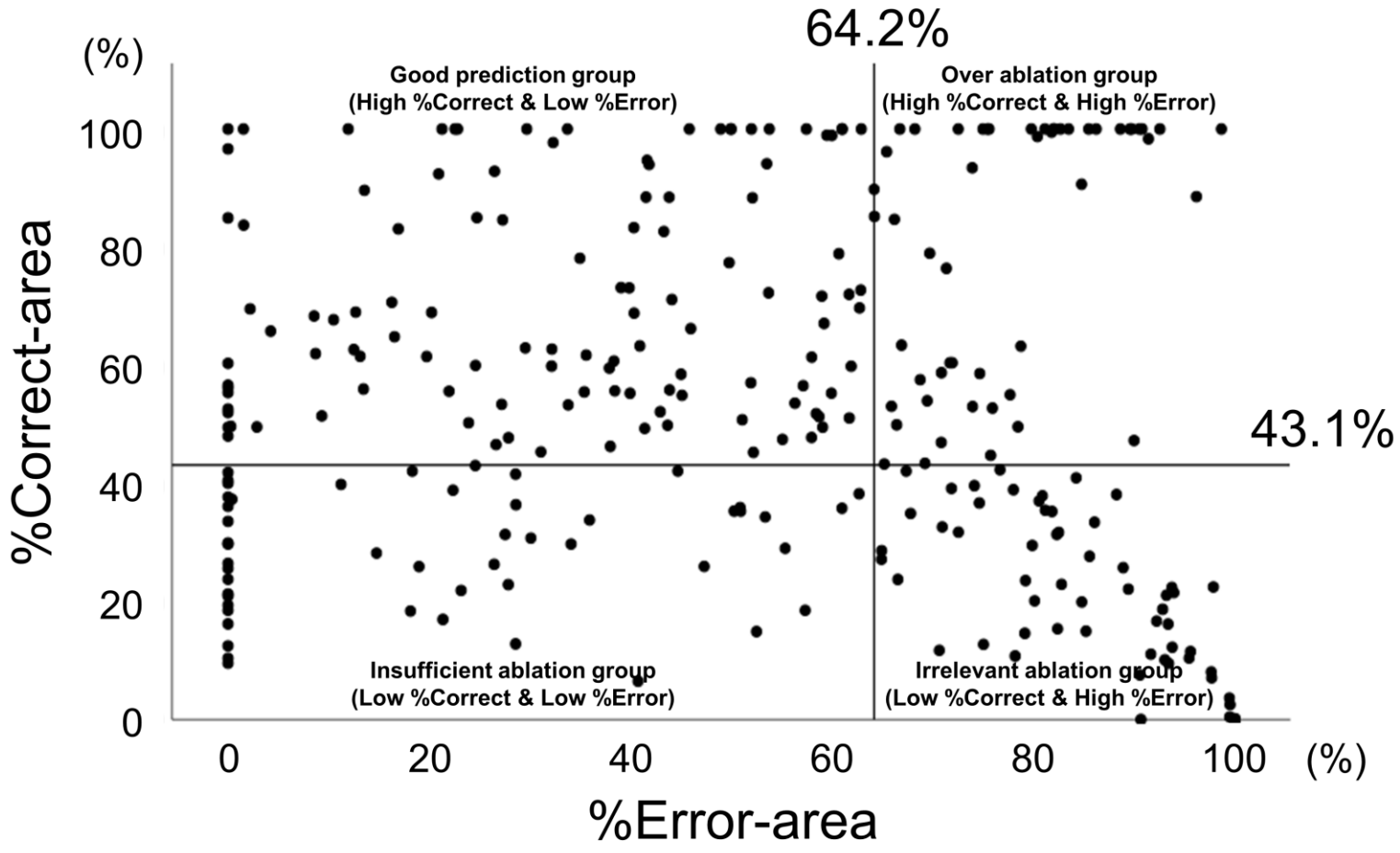
64.2%
(%)
Good prediction group
(High %Correct & Low %Error)
Over ablation group
(High %Correct & High %Error)
100
80
60
40
20
0
%Correct-area
43.1%
Insufficient ablation group
(Low %Correct & Low %Error)
Irrelevant ablation group
(Low %Correct & High %Error)
0
20
40
60
80
100
(%)
%Error-area

Figure 4.

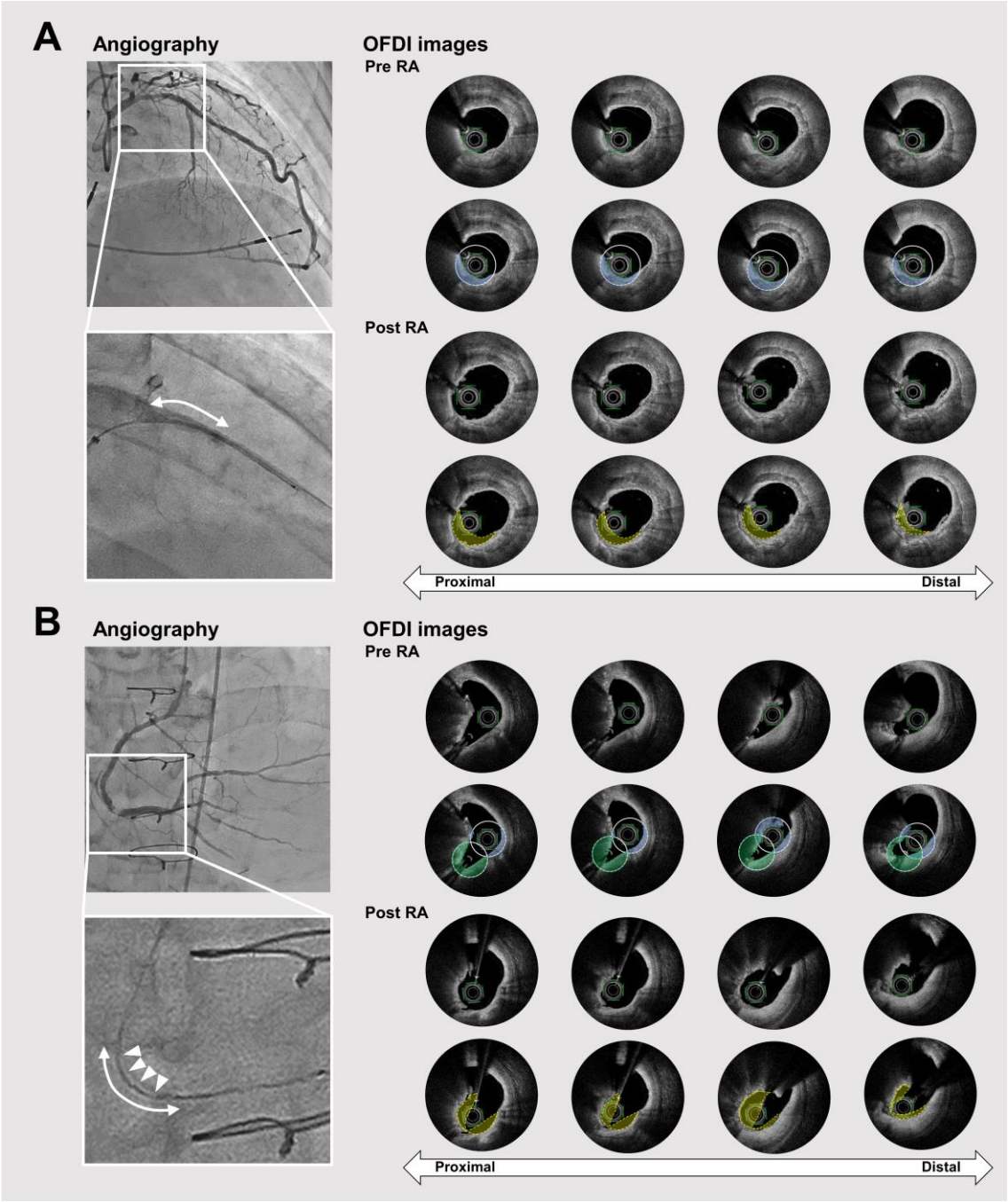
A
Angiography
OFDI images
Pre RA
Post RA
Proximal
Distal
B
Angiography
OFDI images
Pre RA
Post RA
Proximal
Distal

Supplementary Table 1. OFDI measurements before and after rotational atherectomy according to lesion-based analysis.

	n=26
Pre/post-operative lumen measurements	
Pre minimum lumen diameter, mm	0.97 (0.83–1.19)
Pre minimum lumen area, mm^2	1.59 (1.30–2.15)
Post minimum lumen diameter, mm	1.61 (1.45–1.77)
Post minimum lumen area, mm^2	1.98 (1.87–2.16)
Morphology of calcification	
Length of calcification, mm	21.9 (14.8–33.6)
Circumferential calcification, n (%)	9 (34.6)
Eccentric calcification, n (%)	9 (34.6)
Nodular calcification, n (%)	8 (30.8)
RA-related measurement	
Angle-based analysis	
P-angle, ˚	120.0 (78.0–174.6)
A-angle, ˚	80.4 (62.4–139.4)
O-angle, ˚	49.6 (32.0–112.4)
%Correct-angle, %	43.0 (28.0–51.0)
Volume-based analysis	
P-volume, mm^3	6.08 (3.52–10.59)
A-volume, mm^3	6.39 (3.54–12.36)
O-volume, mm^3	2.11 (1.14–4.55)
%Correct-volume, %	50.3 (29.0–57.0)
%Error-volume, %	67.0 (50.0–77.0)
OFDI and wire position	
Minimum distance between the OFDI catheter and intima, mm	0.08 (0.04–0.13)
Minimum distance between the wire and intima, mm	0.25 (0.22–0.29)
Minimum distance between the OFDI catheter and wire, mm	0.04 (0.01–0.07)

Values are expressed as median (interquartile range) or n (%). All variables were calculated as averages at each cross-section per lesion. %Correct-angle was calculated as O-angle divided by P-angle. %Correct-area was calculated as O-area divided by P-area. %Error-area was calculated as A-area minus O-area divided by A-area. P-, A-, and O-volume was calculated by integrating P-, A-, and O-area each cross-section, respectively. %Correct-volume was calculated as O-volume divided by P-volume. %Error-volume was calculated as A-volume minus O-volume

divided by A-volume. Abbreviations: RA, rotational atherectomy; OFDI, optical frequency domain imaging; P-area (volume), predicted ablation area (volume); A-area (volume), actual ablation area (volume); O-area (volume), overlap ablation area (volume); P-angle, angle of predicted ablation area; A-angle, angle of actual ablation area; O-angle, angle of overlap ablation area; %Correct-angle (volume), percentage of correct ablation angle (volume); %Error-volume, percentage of error ablation volume.

Supplementary Table 2. Multiple linear regression analyses for %Correct- and %Error-volume

Variables	%Correct-volume			%Error-volume		
	Standard B	95% CI	P value	Standard B	95% CI	P value
Age	0.08	-0.86 – 1.10	0.790	-0.08	-1.47 – 1.10	0.760
Male	-0.04	-21.3 – 17.8	0.849	0.19	-14.1 – 37.3	0.346
LAD	0.13	-15.2 – 23.7	0.646	-0.27	--38.5 – 12.6	0.291
Floppy wire	-0.12	-21.3 – 13.2	0.617	-0.36-	-40.3 – 5.11	0.117
Judkins type guiding catheter	0.13	-15.3 – 25.1	0.607	0.15	-18.1 – 35.0	0.501
Pre minimum lumen area	-0.01	-14.6 – 14.1	0.968	0.23	-10.2 – 27.5	0.338
Burr / artery ratio	-0.07	-57.2 – 45.9	0.817	-0.20	-91.3 – -44.4	0.465
Mean distance between the OFDI catheter and intima	0.21	-118.1 – 221.8	0.519	-0.26	-315.1 – 131.9	0.390
Mean distance between the wire and intima	-0.17	-114.9 – 62.2	0.529	-0.34	-193.5 – 39.3	0.175
Mean distance between the OFDI catheter and wire	-0.66	-147.6 – 6.0	0.068	0.41	-37.0 – 164.9	0.193
Mean arc of calcium	0.23	-0.08 – 6.69	0.381	0.10	-0.14 – 0.21	0.667
Mean thickness of calcium	-0.38	-46.7 – 6.69	0.128	0.31	-10.7 – 59.6	0.156

Abbreviation: LAD, left anterior descending; OFDI, optical frequency domain imaging.

Supplementary Table 3. Univariate and multivariate logistic regression analyses according to the over ablation group

Variables	Univariate			Multivariate		
	OR	95% CI	*P* value	OR	95% CI	*P* value
LCx	2.52	1.24 – 5.01	0.01			
Extra-support wire	2.80	1.53 – 5.11	0.001	2.21	1.17 – 4.16	0.014
Judkins type guiding catheter	1.13	0.53 – 2.41	0.747			
Pre lumen area	1.23	1.07 – 1.41	0.003			
Burr / lumen ratio	0.16	0.05 – 0.52	0.002			
Distance between the OFDI catheter and intima	7.81	0.78 – 78.6	0.081			
Distance between the wire and intima	0.24	0.04 – 1.33	0.103			
Distance between the OFDI catheter and wire	0.11	0.003 – 3.87	0.23			
Myocardial site calcification	2.01	1.10 – 3.68	0.024			
Arc of calcium	1.00	1.00 – 1.001	0.183			
Thickness of calcium	1.92	0.96 – 3.84	0.065			

Abbreviation: LCx, left circumflex; OFDI, optical frequency domain imaging.

Supplementary Figure 1. Patient flowchart.

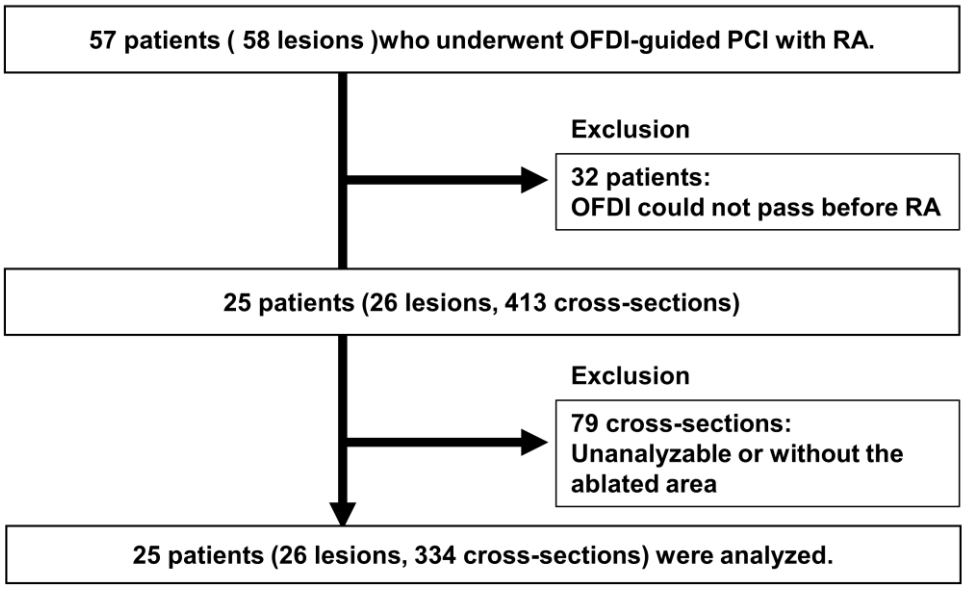

Supplementary Figure 2. Distributions of OFDI findings following rotational atherectomy.

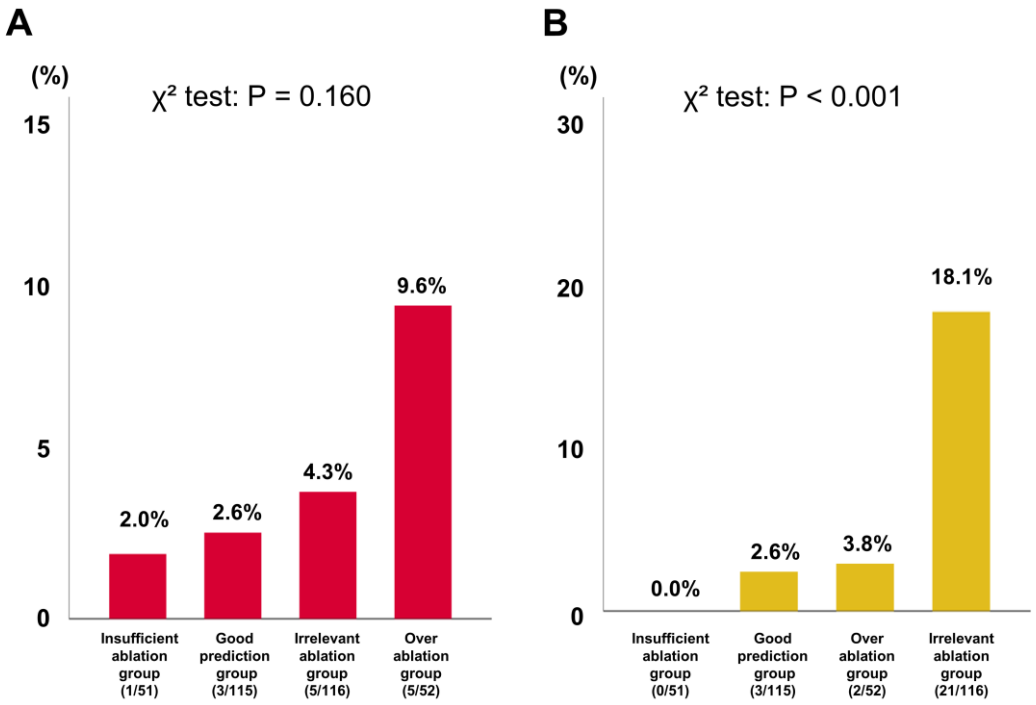

(A) Presence of deep vessel wall injury extending beyond the media following rotational atherectomy. The cross-section with deep vessel wall injury was more frequently observed in the over ablation group (9.6% of cross-sections, 5 of 52 cross-sections, χ^2 test: P = 0.60). (B) Presence of intimal flap outside of the P-area following rotational atherectomy. Cross-sections with intimal flap outside the P-area were more frequently observed in the irrelevant ablation group than the other groups (18.1% of cross-sections, 21 of 116 cross-sections, χ^2 test: P <0.001). OFDI, optical frequency domain imaging.